Rapid Communications

Electron-phonon coupling in the undoped cuprate $YBa_2Cu_3O_6$ estimated from Raman and optical conductivity spectra

D. Farina,[1,2,*] G. De Filippis,[3,†] A. S. Mishchenko,[4,5] N. Nagaosa,[4,6] Jhih-An Yang,[7] D. Reznik,[7,8] Th. Wolf,[9] and V. Cataudella[3]

[1]*Scuola Normale Superiore, Piazza dei Cavalieri 7, I-56126, Pisa, Italy*
[2]*Istituto Italiano di Tecnologia Center for Nanotechnology Innovation @NEST, Piazza San Silvestro 12, I-56127 Pisa, Italy*
[3]*SPIN-CNR and Dipartimento di Scienze Fisiche, Università di Napoli Federico II, I-80126 Napoli, Italy*
[4]*RIKEN Center for Emergent Matter Science (CEMS), 2-1 Hirosawa, Wako, Saitama 351-0198, Japan*
[5]*NRC "Kurchatov Institute," Moscow 123182, Russia*
[6]*Department of Applied Physics, The University of Tokyo, 7-3-1 Hongo, Bunkyo-ku, Tokyo 113, Japan*
[7]*Department of Physics, University of Colorado-Boulder, Boulder, Colorado 80309, USA*
[8]*Center for Experiments on Quantum Materials, University of Colorado-Boulder, Boulder, Colorado 80309, USA*
[9]*Institute for Solid State Physics, Karlsruhe Institute of Technology, D-76021 Karlsruhe, Germany*

(Received 3 December 2017; published 11 September 2018)

We study experimentally the Raman response of the undoped high-T_c parent compound $YBa_2Cu_3O_6$, and give a unified theory of the two-magnon Raman peak and optical conductivity based on the Hubbard-Holstein model with electron-phonon coupling (EPC). The Hubbard model without EPC can qualitatively account for the experimentally observed resonance of the Raman response, but only the Hubbard-Holstein model (i) reproduces the asymmetry of the Raman spectrum, (ii) validates the experimental visibility of the two-magnon peak, and (iii) predicts the correct shape and energy of the lower edge of the charge transfer gap in optical conductivity. A comparison of experiments with the theory gives the EPC strength $\lambda = 0.6$. This result convincingly indicates the vital role of EPC in high-T_c cuprates, providing a clue to the mechanism of high T_c.

DOI: 10.1103/PhysRevB.98.121104

High critical temperature (high-T_c) superconductivity is the phenomenon whose understanding is not only a challenge for the descriptive power of modern theoretical concepts but also bears immense importance for potential numerous applications in many fields of innovative technology. In spite of enormous efforts to understand the physics of high T_c, an opinion on the driving forces leading to the superconducting transition has yet to be adopted [1]. Moreover, there is even no consensus on which types of interactions are crucial for the description of the normal state of high-T_c compounds. It has been adopted by most that the unusual superconductivity of high-T_c compounds cannot be described by conventional Bardeen-Cooper-Schrieffer (BCS) mechanisms based on electron-phonon coupling (EPC) and, hence, one has to assume an important role of the electron-electron interaction (EEI). The emphasis on the EEI in a majority of considered theoretical concepts puts the EPC out of the picture, leaving an impression that the EPC does not play any role in the physics of high-T_c materials.

However, it has been shown by recent studies that the EPC manifests itself in many phenomena [2–11], and it was concluded that one needs both EEI and EPC to describe high-T_c materials [12,13]. The main class of unconventional superconductors are cuprates whose parent undoped compounds are in the Mott insulating antiferromagnetic (AF) state. The doping of these compounds by holes destroys the AF state and induces superconductivity. Recent theoretical studies based on nonperturbative approaches established that the EPC is strongly reflected in the spectroscopy of undoped and weakly doped compounds though its manifestations weaken with hole doping [10,14].

Hence, to address the role of EPC, we focus on undoped compounds where EPC is manifested most clearly, as the basis to construct a theoretical model describing cuprates. This enables the quantitative estimate of the strength of EPC.

To verify the importance of EPC, we calculated the polarization-resolved two-magnon Raman spectrum (RS) and optical conductivity (OC) of undoped ($\delta = 0$) $YBa_2Cu_3O_{6+\delta}$ (YBCO), which is one of the reference high-T_c materials. Our calculations show that a solely EEI-based description, using model parameters required to describe angle-resolved photoemisson spectra of high-T_c compounds, is not successful, whereas the inclusion of rather substantial EPC not only improves the description of both RS and OC but provides a unique possibility to describe both experimental responses within the same unified model.

Model. EEI is introduced in the framework of the extended two-dimensional (2D) effective one-band Hubbard model which has been derived elsewhere [15,16] from the more general three-band description. In addition, we will take into account the coupling between the charge carriers and the vibrational modes of the lattice. The Hamiltonian is

$$H = H_{\mathrm{H}} + H_{\mathrm{PH}} + H_{\mathrm{EPC}}. \quad (1)$$

The first term describes a pure electronic system with a strong on-site Hubbard Coulomb repulsion U, nearest-neighbor

*donato.farina@sns.it
†giuliode@na.infn.it

coupling constant V, and next-nearest-neighbor constant V',

$$H_{\mathrm{H}} = -t \sum_{i,\delta,\sigma} c^{\dagger}_{i+\delta,\sigma} c_{i,\sigma} + U \sum_{i} n_{i,\uparrow} n_{i,\downarrow} + V \sum_{i\delta\sigma\sigma'} n_{i+\delta\sigma} n_{i\sigma'} + V' \sum_{i\delta'\sigma\sigma'} n_{i+\delta'\sigma} n_{i\sigma'}. \quad (2)$$

The vibrational subsystem is described by the out-of-plane dispersionless phonon of apical oxygen ions in YBCO,

$$H_{\mathrm{PH}} = \omega_0 \sum_{i} a^{\dagger}_{i} a_{i}. \quad (3)$$

These couple to charge fluctuations

$$H_{\mathrm{EPC}} = g\omega_0 \sum_{i} (n_i - 1)(a^{\dagger}_{i} + a_i) \quad (4)$$

by on-site Holstein-type EPC whose strength is characterized by the dimensionless 2D coupling constant $\lambda = g^2\omega_0/(4t)$. The values of the parameters entering Eq. (1) have been chosen in agreement with the literature [17–19]. In the present Rapid Communication, we adopt $t = 0.36$ eV, $U = 10t$, $\omega_0 = 0.2t$, $V = 0.2U$, and $V' = 0.1U$ (V and V' have been chosen by assuming a Youkawa-like electron-electron potential) [20]. The antiferromagnetism is controlled by the Heisenberg exchange energy $J = 4t^2/U$ that turns out to be $J = 0.4t$. To calculate the optical response we used exact diagonalization of small systems with semiclassical phonons in an adiabatic approximation (Raman and OC) and with quantum phonons (OC) (see the Supplemental Material [20]). To learn about the importance of EPC we compared the theoretical description with ($\lambda = 0.6$) and without ($\lambda = 0$) EPC. We emphasize that the value $\lambda = 0.6$ restores the correct behavior of OC at very low dopings [21].

Properties where EPC is crucial for describing experiments. In the polarization-resolved Raman response we focused on the bimagnon peak (2M peak) which is located at a Raman shift $\omega = \omega_L - \omega_S$ around 3000 cm^{-1} [22–24]. This shift is the energy loss between incoming laser light with frequency ω_L and outgoing light frequency ω_S. The adopted explanation of the nature of the 2M peak is given by the Chubukov-Frenkel theory [25]. According to this theory, the incident light ω_L creates an electron-hole pair through the electronic gap, which is followed by emission of two bound magnons with the opposite momenta decreasing the electron-hole pair energy by ω. A consequent recombination leads to the emission of light with a smaller frequency ω_S than the incoming light by the Raman shift ω. This process is resonant and the intensity of the 2M peak increases when either ω_L matches the upper edge or when ω_S matches the lower edge of the electronic gap [26,27].

The energy of the 2M peak is mainly determined by EEI, whereas, as shown in Fig. 1, the introduction of EPC significantly improves the similarity of the theoretical description of the Raman response to that measured in experiment [28]. The bimagnon excitation is most pronounced in the Raman response in the $B_{1g} + A_{2g}$ channel where B_{ng} and A_{ng} are irreducible representations of the YBCO crystal point group D_{4h}. This is experimentally detectable by Raman spectroscopy in the $x'y'$ polarization configuration when the incoming $\mathbf{e}_L$ and outgoing $\mathbf{e}_S$ photon polarizations are perpendicular to each other and oriented at 45° with respect to the 2D lattice bonds. The complementary symmetry $A_{1g} + B_{2g}$ or $x'x'$ is experimentally obtained by rotating $\mathbf{e}_S$ to make it parallel to $\mathbf{e}_L$ along the x' direction.

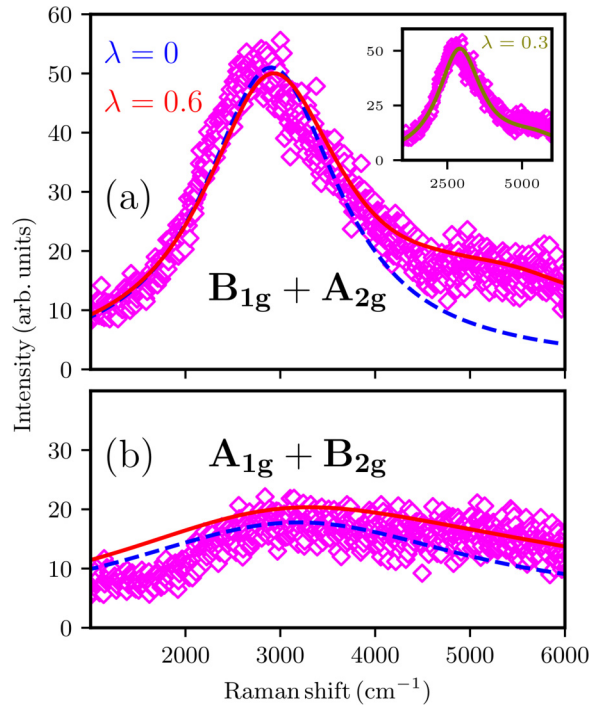

FIG. 1. Calculated Raman signal in (a) $B_{1g} + A_{2g}$ and (b) $A_{1g} + B_{2g}$ symmetries without (dashed blue line) and with (solid red line) EPC ($\lambda = 0.6$). In the inset, we show the calculated Raman signal in $B_{1g} + A_{2g}$ symmetry at $\lambda = 0.3$. Experimental data shown by diamonds were obtained on a single-crystal sample of insulating $YBa_2Cu_3O_{6+x}$ using 3.05-eV incident laser energy on the McPherson triple Raman spectrometer at 300 K.

Without the EPC, in severe contrast with experimental data [24,29], the theoretical 2M peak in the $B_{1g} + A_{2g}$ channel is perfectly symmetric with respect to the bimagnon energy $\omega_{2\mathrm{M}} \sim 2.5J \approx 3000$ cm^{-1}. Inclusion of the EPC cures this discrepancy between the theory and experiment and quantitatively reproduces the asymmetry [see Fig. 1(a); the inset in Fig. 1(a) points out that the best agreement with experimental observations is obtained at $\lambda = 0.6$]. On the other hand, EPC plays a minor role in the $A_{1g} + B_{2g}$ symmetry [see Fig. 1(b)]. However, also in this case, the agreement with experimental observations is improved by the inclusion of charge lattice coupling.

About OC, the very visibility of the 2M peak in the theoretical description is the consequence of EPC (see the inset in Fig. 2). The intensity of the 2M peak in rigid YBCO is suppressed by the point inversion symmetry of the unit cell and only EPC makes the 2M peak visible in principle because phonons break this high symmetry. We note that although the intensity of the bimagnon peak in OC is orders of magnitude weaker than the spectral weight above the gap [21,30], the very presence of this signal, observed in experiment [31], is unambiguous proof of the importance of EPC.

The inclusion of EPC provides other important improvement concerning the shape and the value of the gap in the

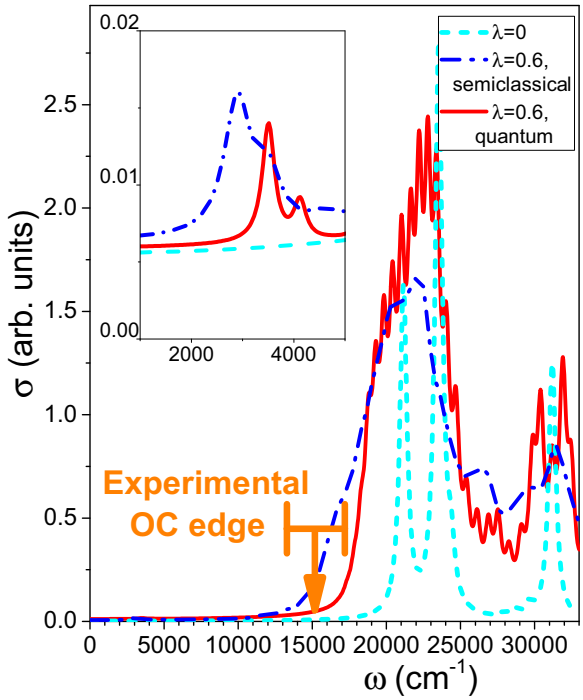

FIG. 2. Theoretical optical conductivity at $\lambda = 0$ (cyan dashed line) and at $\lambda = 0.6$ within the semiclassical (blue dashed-dotted line) and quantum (red solid line) approaches for phonons. The range of OC edge observed in experiments (12 100–16 100 cm^{-1}) is given by the orange error bar with an orange arrow. The inset shows a comparison of OCs in the low-energy window.

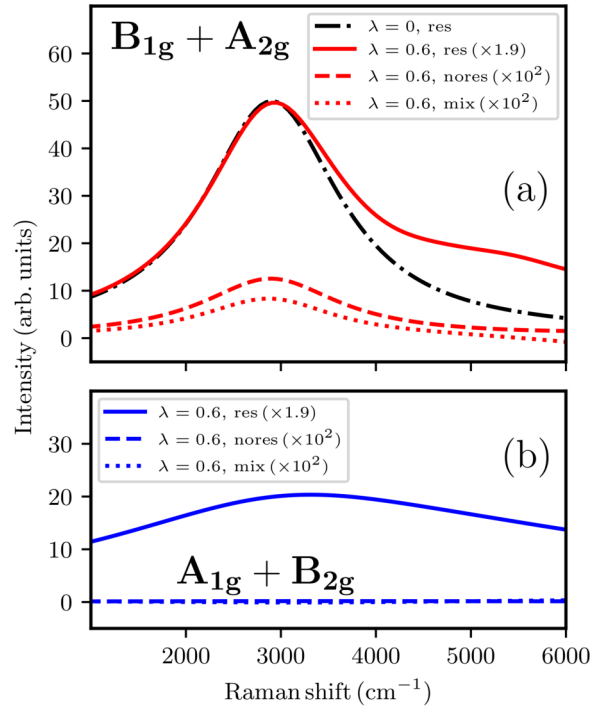

FIG. 3. Resonant (solid line), mixed (dotted line), and nonresonant (dashed line) contributions to the Raman response in (a) $B_{1g} + A_{2g}$ and (b) $A_{1g} + B_{2g}$ symmetries with an electron-phonon interaction ($\lambda = 0.6$) for an incoming laser frequency at resonance. A resonant contribution at $\lambda = 0$ is given in (a) by the black dash-dotted line.

OC (see Fig. 2). Indeed, in the ground state at half filling, Coulomb repulsion forces the electrons to localize, freezing the charge fluctuations. In such a state, the coupling between localized fermions and bosonic excitations, which is mediated by charge dynamics, is strongly suppressed. On the other hand, at the edge of OC, where holons and doublons are formed, charge lattice coupling becomes relevant. EPC moves the edge of the OC to lower energies, building up a characteristic tail just as is reproduced by experiments [32–34]. Here, the main role is played by excitons strongly dressed by phonons. On the other hand, the effect of phonons is less important well inside the absorption band where no polaron can be formed. Nevertheless a simple broadening of the peaks is observed above the charge transfer gap, too.

Properties where EPC is not crucial but plays a big role. Here, we discuss the properties, which are not substantially modified by the inclusion of EPC. To this aim one has to consider the structure of the Raman response and OC. The exact eigenstate representation for the polarization-resolved electronic Raman spectrum at zero temperature as a function of the Raman shift $\omega \equiv \omega_L - \omega_S > 0$ is given by [35,36]

$$I_{\text{Raman}}(\omega; \mathbf{e}_L, \mathbf{e}_S) \propto \frac{\omega_S}{\omega_L} \sum_f |\langle \Psi_f | \mathbf{e}_S^\dagger M \mathbf{e}_L | \Psi_0 \rangle|^2 \times \text{Im} \frac{1}{\omega - E_f + E_0 - i\epsilon}, \quad (5)$$

where $\mathbf{e}_L$ and $\mathbf{e}_S$ are polarizations of the incoming and outgoing light, E_0 and $|\Psi_0\rangle$ are the energy and wave function of the ground state, and E_f and $|\Psi_f\rangle$ are the energies and wave functions of the final states. The matrix elements of the Raman scattering tensor operator

$$\langle \Psi_f | M_{lm} | \Psi_0 \rangle = \langle \Psi_f | \tau_{lm} | \Psi_0 \rangle + \sum_r \left\{ \frac{\langle \Psi_f | j_l | \Psi_r \rangle \langle \Psi_r | j_m | \Psi_0 \rangle}{\omega_L + E_0 - E_r - i\eta} - \frac{\langle \Psi_f | j_m | \Psi_r \rangle \langle \Psi_r | j_l | \Psi_0 \rangle}{\omega_L + E_r - E_f - i\eta} \right\} \quad (6)$$

contain two contributions. The first term is nonresonant, is determined by the Raman stress tensor operator τ_{lm} (see the Supplemental Material [20]), and is insensitive to the incoming photon frequency ω_L. The second one strongly depends on the frequency ω_L, which can resonate only with the difference of the energies of the intermediate $|\Psi_r\rangle$ and ground states, $E_r - E_0$, because of total energy conservation. The resonant term contains the components of the current operator j_l (see the Supplemental Material [20]), and the intermediate states $|\Psi_r\rangle$. The particular structure of the Raman response makes it much more sensitive to symmetry breaking than OC [37,38], namely, to degenerate eigenvalues of the system Hamiltonian. The expression for OC reads as follows,

$$\text{Re}\, \sigma_{xx}^{\text{reg}}(\omega) = \sum_{n \neq 0} \frac{|\langle \Psi_n | j_x | \Psi_0 \rangle|^2}{E_n - E_0} \text{Re} \left[i \left(\frac{1}{\omega + i\delta - E_n + E_0} - \frac{1}{\omega + i\delta + E_n - E_0} \right) \right]. \quad (7)$$

The dominant contribution to the Raman scattering, both with and without EPC, comes from the resonant contribution

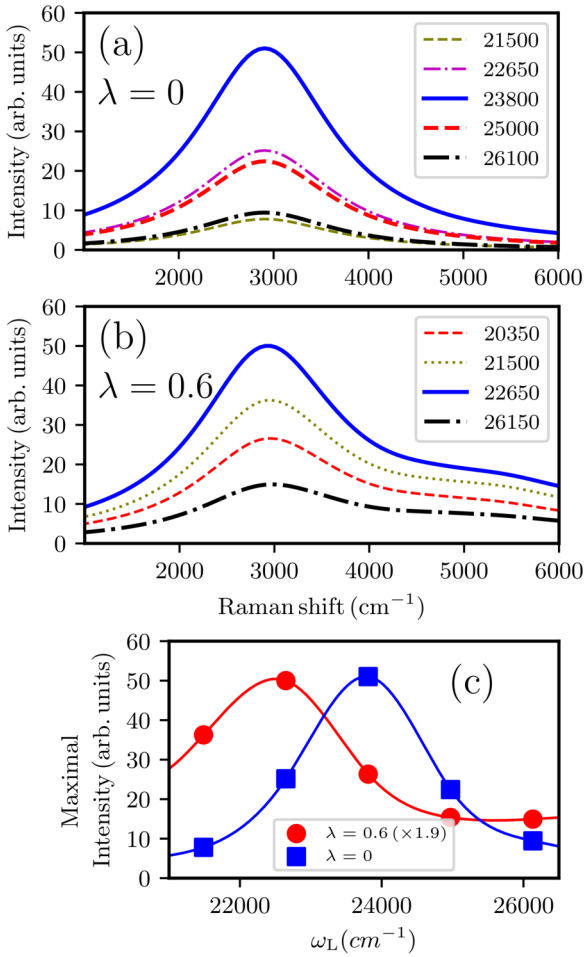

FIG. 4. Resonant behavior of the Raman response in $B_{1g} + A_{2g}$ symmetry (a) without and (b) with electron-phonon coupling ($\lambda = 0.6$). The incoming laser frequencies ω_L in cm^{-1} are given in the figure legends. (c) shows the dependence of the maximal Raman signal intensity on the incoming laser frequency ω_L.

(see Fig. 3, where different terms of the Raman response are compared for $\lambda = 0.6$). Figure 3(a) compares resonant contributions at $\lambda = 0.6$ and $\lambda = 0$. One can conclude that the EPC is responsible for the experimentally observed asymmetry of the 2M peak in $B_{1g} + A_{2g}$ symmetry and that EPC mostly affects the resonant contribution. This stems from the observation that the resonant contribution involves states at the edge of OC, where holons and doublons are formed and EPC plays a significant role.

The resonant behavior is observed both with and without EPC (Fig. 4). In both cases, comparing Figs. 4(c) and 2, one concludes that the resonant contribution is maximal when the incident frequency ω_L matches the maximum of the OC above the charge transfer gap. However, the resonance is much broader when EPC is included, which is closer to the experiment [39].

We emphasize that RS are often discussed in literature within the framework of the Fleury-London theory based on the coupling between the light and the spin system in the Heisenberg model [40]. However, these approaches do not reproduce resonant scattering occurring when the frequency of the incoming light is comparable to the charge transfer gap. In order to recover the experimental resonance one has to take into account the full Hubbard model [17].

Conclusion. We compared the capabilities of the extended Hubbard and extended Hubbard-Holstein models to give a unified description of the Raman response and optical conductivity of high-T_c superconductors on the example of the prototypical undoped compound ($\delta = 0$) $YBa_2Cu_3O_{6+\delta}$. We showed that both models can explain the experimentally observed resonant nature of the Raman response. However, we found that the extended Hubbard-Holstein model, including electron-phonon coupling, gives a better description of the experimental data. First, the Hubbard-Holstein model, in contrast with the pure Hubbard model, reproduces the experimentally observed asymmetry of the Raman spectrum. Second, the presence of the electron-phonon coupling is manifested in the experimental visibility of the two-magnon peak in optical conductivity. Finally, the Hubbard-Holstein model predicts the correct positions of peaks both in the Raman response and optical conductivity with the same parameters, i.e., it provides a unified description of two spectral properties in a situation where a pure Hubbard model fails.

This work was funded by ImPACT Program of Council for Science, Technology and Innovation (Cabinet Office, Government of Japan). Work at the University of Colorado was supported by the NSF under Grant No. DMR-1709946. N.N. was supported by Ministry of Education, Culture, Sports, Science, and Technology Grants No. JP24224009 and No. JP26103006, the Impulsing Paradigm Change through Disruptive Technologies Program of Council for Science, Technology and Innovation (Cabinet Office, Government of Japan), and Core Research for Evolutionary Science and Technology (CREST) Grant No. JPMJCR16F1.

[1] P. A. Lee, N. Nagaosa, and X. G. Wen, Rev. Mod. Phys. **78**, 17 (2006).
[2] T. P. Devereaux, A. Virosztek, and A. Zawadowski, Phys. Rev. B **51**, 505 (1995).
[3] G. Khaliullin and P. Horsch, Physica C (Amsterdam) **282**, 1751 (1997).
[4] O. Rösch and O. Gunnarsson, Phys. Rev. Lett. **92**, 146403 (2004).
[5] A. S. Mishchenko and N. Nagaosa, Phys. Rev. Lett. **93**, 036402 (2004).
[6] O. Rösch and O. Gunnarsson, Phys. Rev. Lett. **93**, 237001 (2004).

[7] O. Rösch, O. Gunnarsson, X. J. Zhou, T. Yoshida, T. Sasagawa, A. Fujimori, Z. Hussain, Z. X. Shen, and S. Uchida, Phys. Rev. Lett. **95**, 227002 (2005).

[8] G. Sangiovanni, O. Gunnarsson, E. Koch, C. Castellani, and M. Capone, Phys. Rev. Lett. **97**, 046404 (2006).

[9] V. Cataudella, G. De Filippis, A. S. Mishchenko, and N. Nagaosa, Phys. Rev. Lett. **99**, 226402 (2007).

[10] A. S. Mishchenko, N. Nagaosa, Z. X. Shen, G. De Filippis, V. Cataudella, T. P. Devereaux, C. Bernhard, K. W. Kim, and J. Zaanen, Phys. Rev. Lett. **100**, 166401 (2008).

[11] F. Novelli, G. De Filippis, V. Cataudella, M. Esposito, I. V. Kausel, F. Cilento, E. Sindici, A. Amaricci, C. Giannetti, D. Prabhakaran, S. Wall, A. Perucchi, S. Dal Conte, G. Cerullo, M. Capone, A. Mishchenko, M. Grüninger, N. Nagaosa, F. Parmigiani, and D. Fausti, Nat. Commun. **5**, 5112 (2014).

[12] O. Gunnarsson and O. Rösch, J. Phys.: Condens. Matter **20**, 043201 (2008).

[13] A. S. Mishchenko, Phys. Usp. **52**, 1193 (2009).

[14] A. S. Mishchenko, N. Nagaosa, K. M. Shen, Z. X. Shen, X. J. Zhou, and T. P. Devereaux, Europhys. Lett. **95**, 57007 (2011).

[15] L. F. Feiner, J. H. Jefferson, and R. Raimondi, Phys. Rev. B **53**, 8751 (1996).

[16] M. E. Simon, A. A. Aligia, and E. R. Gagliano, Phys. Rev. B **56**, 5637 (1997).

[17] T. Tohyama, H. Onodera, K. Tsutsui, and S. Maekawa, Phys. Rev. Lett. **89**, 257405 (2002).

[18] G. Seibold, C. Castellani, C. Di Castro, and M. Grilli, Phys. Rev. B **58**, 13506 (1998).

[19] S. Raghu, E. Berg, A. V. Chubukov, and S. A. Kivelson, Phys. Rev. B **85**, 024516 (2012).

[20] See Supplemental Material at http://link.aps.org/supplemental/10.1103/PhysRevB.98.121104 for descriptions of the methods used in the calculations, and justification of the parameters of the model, which includes Refs. [41–46].

[21] G. De Filippis, V. Cataudella, E. A. Nowadnick, T. P. Devereaux, A. S. Mishchenko, and N. Nagaosa, Phys. Rev. Lett. **109**, 176402 (2012).

[22] D. Reznik, M. V. Klein, W. C. Lee, D. M. Ginsberg, and S. W. Cheong, Phys. Rev. B **46**, 11725 (1992).

[23] M. Yoshida, S. Tajima, N. Koshizuka, S. Tanaka, S. Uchida, and T. Itoh, Phys. Rev. B **46**, 6505 (1992).

[24] G. Blumberg, P. Abbamonte, M. V. Klein, W. C. Lee, D. M. Ginsberg, L. L. Miller, and A. Zibold, Phys. Rev. B **53**, R11930 (1996).

[25] A. V. Chubukov and D. M. Frenkel, Phys. Rev. Lett. **74**, 3057 (1995).

[26] D. K. Morr and A. V. Chubukov, Phys. Rev. B **56**, 9134 (1997).

[27] E. Hanamura, N. T. Dan, and Y. Tanabe, Phys. Rev. B **62**, 7033 (2000).

[28] The polarization-resolved electronic Raman spectrum intensity at zero temperature as a function of the Raman shift is given in Eqs. (5) and (6) up to a factor. In order to fit the experimental observations in Fig. 1, we have chosen two different factors for $\lambda = 0$ and $\lambda = 0.6$. The two factors differ by 1.9. By varying the incoming frequency (in order to obtain the resonant behavior of the Raman response in the $B_{1g} + A_{2g}$ symmetry shown in Fig. 4), this multiplicative contribution has not been changed. The same factors have been used also in the Supplemental Material.

[29] N. Chelwani, A. Baum, T. Bohm, M. Opel, F. Venturini, L. Tassini, A. Erb, H. Berger, L. Forró, and R. Hackl, Phys. Rev. B **97**, 024407 (2018).

[30] J. Lorenzana and G. A. Sawatzky, Phys. Rev. B **52**, 9576 (1995).

[31] J. D. Perkins, J. M. Graybeal, M. A. Kastner, R. J. Birgeneau, J. P. Falck, and M. Greven, Phys. Rev. Lett. **71**, 1621 (1993).

[32] J. Orenstein, G. A. Thomas, A. J. Millis, S. L. Cooper, D. H. Rapkine, T. Timusk, L. F. Schneemeyer, and J. V. Waszczak, Phys. Rev. B **42**, 6342 (1990).

[33] G. Yu, C. H. Lee, D. Mihailovic, A. J. Heeger, C. Fincher, N. Herron, and E. M. McCarron, Phys. Rev. B **48**, 7545 (1993).

[34] S. L. Cooper, A. L. Kotz, M. A. Karlow, M. V. Klein, W. C. Lee, J. Giapintzakis, and D. M. Ginsberg, Phys. Rev. B **45**, 2549 (1992).

[35] B. S. Shastry and B. I. Shraiman, Phys. Rev. Lett. **65**, 1068 (1990).

[36] T. P. Devereaux and R. Hackl, Rev. Mod. Phys. **79**, 175 (2007).

[37] Y. Gallais and I. Paul, C. R. Phys. **17**, 113 (2016).

[38] P. Massat, D. Farina, I. Paul, S. Karlsson, P. Strobel, P. Toulemonde, M. A. Méasson, M. Cazayous, A. Sacuto, S. Kasahara *et al.*, Proc. Natl. Acad. Sci. USA **113**, 9177 (2016).

[39] G. Blumberg, R. Liu, M. V. Klein, W. C. Lee, D. M. Ginsberg, C. Gu, B. W. Veal, and B. Dabrowski, Phys. Rev. B **49**, 13295 (1994).

[40] A. W. Sandvik, S. Capponi, D. Poilblanc, and E. Dagotto, Phys. Rev. B **57**, 8478 (1998), and references therein.

[41] E. Dagotto, R. Joynt, A. Moreo, S. Bacci, and E. Gagliano, Phys. Rev. B **41**, 9049 (1990).

[42] G. De Filippis, V. Cataudella, A. S. Mishchenko, and N. Nagaosa, Phys. Rev. Lett. **99**, 146405 (2007).

[43] K. Shinjo and T. Tohyama, Phys. Rev. B **96**, 195141 (2017).

[44] D. J. J. Marchand, G. De Filippis, V. Cataudella, M. Berciu, N. Nagaosa, N. V. Prokof'ev, A. S. Mishchenko, and P. C. E. Stamp, Phys. Rev. Lett. **105**, 266605 (2010).

[45] G. De Filippis, V. Cataudella, A. S. Mishchenko, and N. Nagaosa, Phys. Rev. B **85**, 094302 (2012).

[46] B. S. Shastry and B. Sutherland, Phys. Rev. Lett. **65**, 243 (1990).